

R-SYMMETRIC SUPER-QCD AT THE NLO*

WOJCIECH KOTLARSKI, SEBASTIAN LIEBSCHNER

Institute for Nuclear and Particle Physics, TU Dresden
Zellescher Weg 19, 01069 Dresden, Germany

(Received November 8, 2017)

We report on the recent calculation of the next-to-leading order, super-QCD corrections to the squark–(anti)squark pair production in the Minimal *R*-symmetric Supersymmetric Standard Model. The emphasis is put on highlighting differences compared to the Minimal Supersymmetric Standard Model. Phenomenological consequences for the LHC are also briefly discussed.

DOI:10.5506/APhysPolB.48.2347

1. Introduction

With the Large Hadron Collider being less than two years away from its second long technical shutdown, there are still no signs of new physics on the horizon. Other than a few (yet) statistically insignificant “anomalies” (see, for example, [1] for the recent one), all measurements agree well with predictions of the Standard Model.

This puts a lot of models which promised to solve the problems of the Standard Model in an uncomfortable situation. It is especially true for supersymmetry, where heavy stop squarks lead to significant fine tuning.

In recent years, this situation drew attention towards non-minimal SUSY models. In the simplest extensions, like the NMSSM, the SQCD sector remains unmodified compared to the MSSM. More involved extensions can contain particles such as Dirac gluinos or even exotic states like leptoquarks.

Between those and other proposals, the Minimal *R*-symmetric Supersymmetric Standard Model (MRSSM) [2] presents a nice middle ground. It provides a consistent framework for testing SUSY characteristics not present in the MSSM (or even the NMSSM), while remaining less baroque than, for example, the E_6 SSM.

* Presented by W. Kotlarski at the XLI International Conference of Theoretical Physics “Matter to the Deepest”, Podlesice, Poland, September 3–8, 2017.

2. The Minimal R -symmetric Supersymmetric Standard Model

Table I lists the strongly interacting particles of the model, which is what we exclusively focus on in this note. The field content of the MRSSM is enlarged compared to the MSSM to accommodate a Dirac mass term for the gluino. Hence, it requires an additional Weyl spinor coming from a chiral adjoint superfield \widehat{O} . To preserve supersymmetry, this spinor comes accompanied by two real scalar fields, called sgluons and denoted by O_p and O_s .

TABLE I

Strongly interacting fields of the MRSSM, together with the R -charges of the component fields. The superfield in the last line is absent in the MSSM. It comprises the right-handed component of the Dirac gluino and two real sgluons.

Superfield		Boson	Fermion		
Left-handed (s)quark	\widehat{Q}_L	\tilde{q}_L	1	q_L	0
Right-handed (s)quark	\widehat{Q}_R	\tilde{q}_R^\dagger	1	\bar{q}_R	0
Gluon vector superfield	\widehat{V}	g	0	\tilde{g}_L	+1
Adjoint chiral superfield	\widehat{O}	O	0	\tilde{g}_R	-1

The characteristic feature of the MRSSM is the presence of an unbroken R -symmetry [3, 4]. For comparison with the MSSM, one can treat matter parity of the MSSM, defined as $M_p = (-1)^{3(B-L)}$, as a Z_2 subgroup of the R -symmetry $U(1)_R = e^{i\alpha R}$, obtained by restricting $\alpha = \pi$. For $\alpha = \pi$ and $R \in \mathbb{Z}$, the result is always ± 1 , with left- and right-handed squark fields transforming with a minus sign under R -parity. In the MRSSM, this is no longer true, due to an unrestricted α . Therefore, for a generic α , only a left–right combination transforms as an R -symmetric singlet. Hence, left–left and right–right squark pair production is forbidden. Analogously, the left–right squark–antisquark production is also forbidden, while the left–left and right–right production is allowed.

Therefore, on a phenomenological level, the difference between MSSM and MRSSM boils down to three things:

- the presence of Dirac gluinos, reflected either in their direct production or their contribution to squark pair production as a t -channel mediator;
- the reduction of the inclusive (summed over left and right states) production cross section for squark pairs;
- the presence of sgluons.

Since the LHC is hinting that gluinos (if they exist) must be heavy, we are focusing here on the (anti)squark production¹. We consider two scenarios, called BMP1 and BMP2, where $m_q = 1.5$ TeV, $m_{O_p} = m_O = 5$ TeV and $m_{\tilde{g}} = 1$ TeV (BMP1) or 2 TeV (BMP2), with m_O being a soft-breaking mass parameter. The mass of the scalar sgluon O_s receives additional D -term contributions raising its mass to, for example, $m_{O_s} = \sqrt{m_O^2 + 4m_{\tilde{g}}^2} \approx 5.4$ TeV in the case of BMP1.

In Fig. 1, we plot the leading order cross sections for the 13 TeV LHC, for the MSSM and MRSSM. It illustrates the reduction in $\tilde{q}\tilde{q}$ production cross section and increase in the $\tilde{g}\tilde{g}$ one for the MRSSM compared to the MSSM discussed in this section.

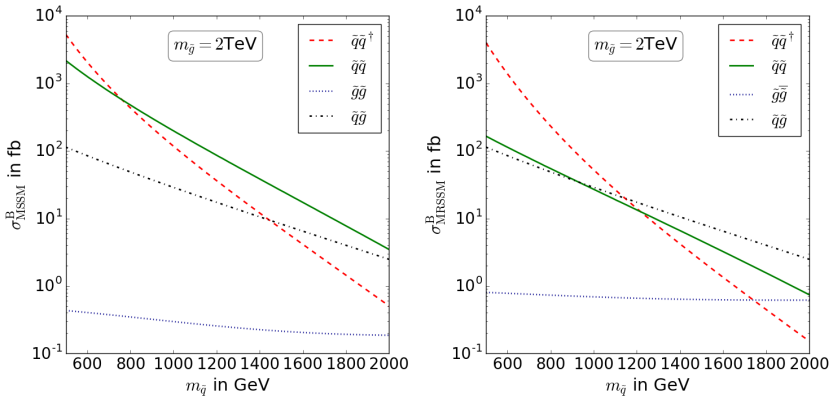


Fig. 1. Comparison of the hadronic cross sections for $\sqrt{S} = 13$ TeV LHC for squark and gluino production in the function of the squark mass. Different flavours (excluding stops), “chiralities” and charge conjugates are summed over.

3. Virtual corrections

Beyond the leading order, virtual corrections for $qq \rightarrow \tilde{q}\tilde{q}$, $gg \rightarrow \tilde{q}\tilde{q}^\dagger$ and $q\bar{q} \rightarrow \tilde{q}\tilde{q}^\dagger$ processes need to be computed. In order to extract UV- and IR-divergencies, we regularise them dimensionally. Since there is no regularisation scheme which respects SUSY and is, at the time, in accordance with the standard definition of PDFs, we perform the calculation in two different regularisation schemes:

1. Dimensional regularisation (HV in the notation of Ref. [5]) is compatible with the standard definition of PDF sets. It requires the introduction of SUSY-restoring counterterms, though.

¹ We are mainly interested in a comparison to the MSSM. Hence, we also do not consider an MRSSM specific signature of sgluon production here.

2. Dimensional reduction (FDH in the notation of Ref. [5]) preserves SUSY, but comes with the necessity of introducing a finite shift in α_s and a transformation of the squared amplitudes from FDH to HV. The latter is performed with universal formulae and is required as the real correction are calculated in HV and the convolution with PDF sets also requires HV.

We have computed the required renormalisation constants (see Ref. [6]) in both HV and FDH, using vanishing quark masses (except for the top quark) and degenerate squark masses. Mass and field renormalisation constants are calculated in the on-shell scheme, while the strong coupling is treated such, that heavy particles decouple.

3.1. Method 1: HV and Passarino–Veltman reduction

Since HV breaks SUSY, we introduce a SUSY-restoring counterterm. In the case at hand, it is sufficient to only shift the renormalisation constant of the SUSY-analogue of the gauge coupling, *i.e.* the coupling $\delta\hat{g}_s$ of the $q\tilde{q}\tilde{g}$ -vertex: $\delta\hat{g}_s = \delta g_s + \delta g^{\text{restore}}$. The SUSY-restoring constant reads

$$\delta g^{\text{restore}} = \frac{g_s^3}{16\pi^2} \left(\frac{2C_A}{3} - \frac{C_F}{2} \right) \quad (1)$$

and is the same in the MSSM, because SUSY breaking effects originate from gluon contributions which are identical in both models.

To implement the calculation, we used an MRSSM model file generated by SARAH [7–10] to generate and process amplitudes with the aid of the Mathematica packages FeynArts [11] and FormCalc [12, 13]. Counterterm Feynman rules and renormalisation constants have been added by hand into the model file.

3.2. Method 2: FDH and integrated reduction approach

In this approach, we implement the transition rules [14, 15] for squared amplitudes from FDH to HV and conversion of δg_s from FDH to HV in GoSam 2 [16, 17]. Model details are passed to GoSam using the UFO interface [18]. The renormalisation of the MRSSM has been added by hand to GoSam. The counterterms are implemented using OneLoop for the loop functions and added to the `matrix.f90` template in the GoSam interface. The exact counterterm structure has to be fixed once after generating the considered process with GoSam.

4. Real corrections

The infrared divergences from the virtual amplitude cancel against divergences present in real-emission diagrams. The real corrections are calculated using two, alternative ways, *i.e.* the two-cut phasespace slicing (TCPSS) method [19] and the FKS subtraction [20, 21]. The TCPSS relies on two arbitrary (but small) parameters δ_s, δ_c . We compare the two approaches in Fig. 2 (left), where we plot the TCPSS result as a function of δ_c . The FKS result is independent of this parameter, and for a sufficiently small value of δ_s , both results are in agreement. For diagrams involving on-shell resonances we employ a diagram removal procedure [22].

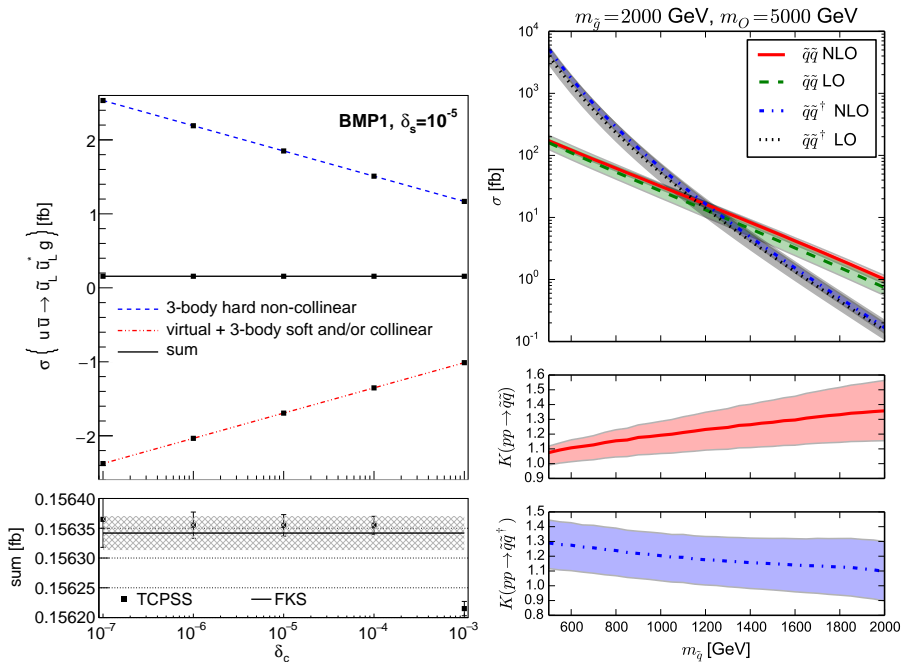


Fig. 2. Left: Dependence of the two-cut phasespace slicing result on the slicing parameter δ_c . For comparison, we include the FKS result. Right: Leading and Next-to-Leading order cross sections for squark pair production (summed as in Fig. 1). The lower panels show K -factors together with combined scale and PDF uncertainties.

5. Results

In Fig. 2 (right), we show the equivalent of the plot in Fig. 1 after adding NLO corrections. The lower subplots in Fig. 2 (right) show K -factors, together with combined scale and PDF uncertainties. The K -factors are moderate, ranging up to 50% for squark masses of 1 TeV and are what one would expect from NLO corrections to a QCD process.

The importance of the result can only be appreciated after comparing it with the MSSM. We do this in two ways. In Fig. 3 (left), we plot the ratio of MRSSM and MSSM K -factors for the $pp \rightarrow \tilde{u}_L \tilde{u}_R$ process in function of gluino and common squark masses. The difference between K -factors is moderate, in the range of $\pm 10\%$. In Fig. 3 (right), we redo the plot after summing over squark “chiralities” (obviously, only the MSSM K -factor is affected). Here, the difference is much more pronounced. The figure emphasizes the danger of taking inclusive MSSM squark K -factors and applying them to the MRSSM.

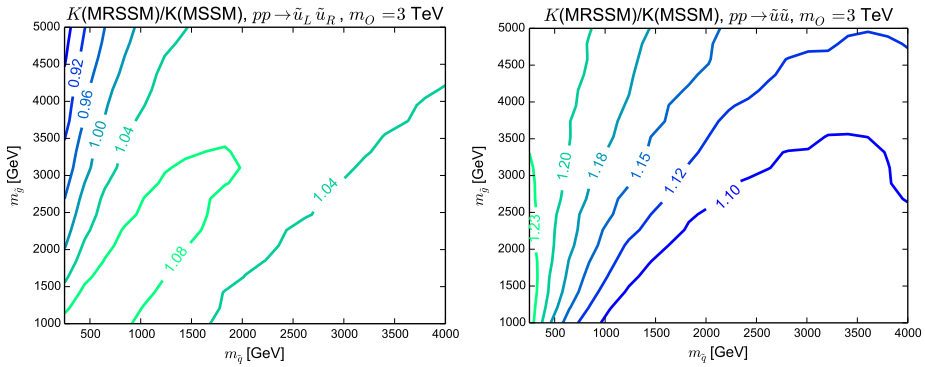


Fig. 3. Ratios of MRSSM to MSSM K -factors in the $m_{\tilde{g}}-m_{\tilde{q}}$ plane. Left figure compares only $\tilde{u}_L \tilde{u}_R$ production, while the right one sums the MSSM result over different squark “chiralities”.

Finally, the differential cross sections in two selected observables, that is transverse momentum and pseudorapidity of the hardest squark, are shown in Fig. 4. Here, the global and differential K -factors agree well in the range of squark’s $p_T \in [500, 1500]$ GeV and $|\eta| \lesssim 2$.

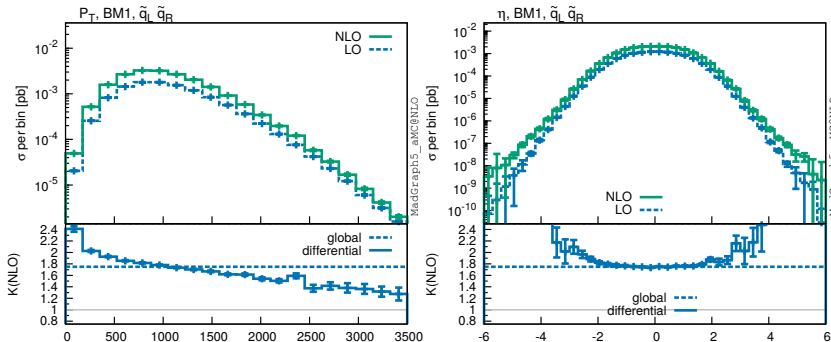


Fig. 4. Differential distributions of hardest squark’s p_T and η .

6. Conclusions

The MRSSM is an interesting alternative to the MSSM. It is a good testing ground, both for theorists and experimentalists, to study features of SUSY not present in the MSSM.

In this work, we have reported on a recent calculation of NLO super-QCD corrections in the MRSSM to squark pair productions at the LHC. We hope that the progress in the precision calculations in the beyond the minimal SUSY phenomenology will encourage experimentalist to perform studies dedicated to this class of models.

We thank Philip Diessner and Dominik Stöckinger with whom the original work on which this paper is based on was performed. This research was supported in part by the German Research Foundation (DFG) under grants number SI 2009/1-1 and STO 876/4-1, the National Science Centre, Poland (NCN) under contract UMO-2015/18/M/ST2/00518 (2016–2019) and the PL-Grid Infrastructure.

REFERENCES

- [1] CMS Collaboration, CMS-PAS-HIG-17-013 report.
- [2] G.D. Kribs, E. Poppitz, N. Weiner, *Phys. Rev. D* **78**, 055010 (2008) [arXiv:0712.2039 [hep-ph]].
- [3] A. Salam, J.A. Strathdee, *Nucl. Phys. B* **87**, 85 (1975).
- [4] P. Fayet, *Nucl. Phys. B* **90**, 104 (1975).
- [5] A. Signer, D. Stöckinger, *Nucl. Phys. B* **808**, 88 (2009) [arXiv:0807.4424 [hep-ph]].
- [6] P. Diessner, W. Kotlarski, S. Liebschner, D. Stöckinger, *J. High Energy Phys.* **1017**, 142 (2017) [arXiv:1707.04557 [hep-ph]].
- [7] F. Staub, *Comput. Phys. Commun.* **181**, 1077 (2010) [arXiv:0909.2863 [hep-ph]].
- [8] F. Staub, *Comput. Phys. Commun.* **182**, 808 (2011) [arXiv:1002.0840 [hep-ph]].
- [9] F. Staub, *Comput. Phys. Commun.* **184**, 1792 (2013) [arXiv:1207.0906 [hep-ph]].
- [10] F. Staub, *Comput. Phys. Commun.* **185**, 1773 (2014) [arXiv:1309.7223 [hep-ph]].
- [11] T. Hahn, *Comput. Phys. Commun.* **140**, 418 (2001) [arXiv:hep-ph/0012260].
- [12] B. Chokoufe Nejad, T. Hahn, J.N. Lang, E. Mirabella, *J. Phys.: Conf. Ser.* **523**, 012050 (2014) [arXiv:1310.0274 [hep-ph]].

- [13] T. Hahn, M. Pérez-Victoria, *Comput. Phys. Commun.* **118**, 153 (1999) [arXiv:hep-ph/9807565].
- [14] Z. Kunszt, A. Signer, Z. Trócsányi, *Nucl. Phys. B* **411**, 397 (1994) [arXiv:hep-ph/9305239].
- [15] S. Catani, M.H. Seymour, Z. Trócsányi, *Phys. Rev. D* **55**, 6819 (1997) [arXiv:hep-ph/9610553].
- [16] G. Cullen *et al.*, *Eur. Phys. J. C* **72**, 1889 (2012) [arXiv:1111.2034 [hep-ph]].
- [17] G. Cullen *et al.*, *Eur. Phys. J. C* **74**, 3001 (2014) [arXiv:1404.7096 [hep-ph]].
- [18] C. Degrande *et al.*, *Comput. Phys. Commun.* **183**, 1201 (2012) [arXiv:1108.2040 [hep-ph]].
- [19] B.W. Harris, J.F. Owens, *Phys. Rev. D* **65**, 094032 (2002) [arXiv:hep-ph/0102128].
- [20] S. Frixione, Z. Kunszt, A. Signer, *Nucl. Phys. B* **467**, 399 (1996) [arXiv:hep-ph/9512328].
- [21] S. Frixione, *Nucl. Phys. B* **507**, 295 (1997) [arXiv:hep-ph/9706545].
- [22] S. Frixione *et al.*, *J. High Energy Phys.* **0807**, 029 (2008) [arXiv:0805.3067 [hep-ph]].